19

Gold nanostars for SERS mapping of tissues using red medical lasers

© V.O. Svinko, A.I. Shevchuk, A.N. Smirnov, D.V. Makeeva, E.V. Solovyeva

Insitute of Chemistry, Saint Petersburg University,
198504 St. Petersburg, Russia

e-mail: e.solovieva@spbu.ru

Received August 03, 2022
Revised August 03, 2022
Accepted August 11, 2022

Star-shaped gold nanoparticles modified with cyanine 5.5 derivatives were studied as optical tags for bioimaging by surface-enhanced Raman scattering (SERS). Obtained tags showed a plasmon resonance band at 640 nm in the absorption spectra which ensures them a maximum efficiency when excited by red lasers. SERS measurements were carried out for the modified particles in the solution phase and after incubation with the PANC-1 cell line. The SERS spectra of the solutions revealed a characteristic signal of cyanine 5.5 amino derivative in the range of $100-1000\,cm^{-1}$, where there is no high fluorescent background. In cell samples, the SERS spectrum of the dye was recorded from the cytoplasm and was not detected outside the cells. In order to confirm the intracellular localization of the tags, the SERS spectra were also scanned in height. The test on cytotoxicity showed that the studied tags are not toxic in the concentration range from 0.05 to 1 mg/l on atomic gold.

Keywords: surface-enhanced Raman scattering, gold nanostar, cyanine, optical tags, bioimaging

DOI: 10.21883/EOS.2022.10.54872.3709-22

Introduction

Lasers with a wavelength in the range of 630−660 nm are widely used in various fields of medicine: in molecular tomography, dermatology, surgery and ophthalmology. The advantages of red lasers lie in their rather high efficiency and safety [1]. The red beam is capable of penetrating into human tissues to a depth of 0.1 to 5 mm, so such lasers can be used to diagnose and treat various superficial neoplasms. The development of selectively targeted optical labels excited by red lasers is of great interest for the treatment of certain types of cancer [2]. In particular, such optical agents have already been proposed for the treatment of melanoma [3] and the detection of breast cancer [4].

Giant Raman spectroscopy (GRS) of light is one of the most actively developing methods of bioimaging. In this method, functionalized plasmonic nanoparticles (NPs) or systems of the „core−shell"type are often used as markers. GRS spectroscopy can be implemented for bioimaging purposes in *in vitro*, *in vivo* and *ex vivo* modes, and its higher selectivity and sensitivity are the main advantages over fluorescence microscopy [5,6]. Recently, quite interesting studies have appeared on the development of Raman tomography [7], which open up even broader prospects for the practical application of the GRS method. However, the already existing works on GRS mapping of biological samples demonstrate the possibility of obtaining sufficiently accurate volumetric images of uneven objects at a depth of up to 100 nm [8,9].

The potential of gold nanoparticles as markers for bioimaging and photothermal agents has been repeatedly demonstrated in many works [10]. However, the morphology of the particles used should be chosen based on the planned practical applications of specific markers. Gold nanostars (GNSs) have an absorption band in the region of 620−650 nm [11]. Gold nanostars do not have a high anisotropy, in contrast to the well-known nanorods [12], which have the main absorption band at higher wavelengths, but at the same time differ significantly from spherical NPs, which absorb in the region up to 600 nm [13]. It should be noted that the size and shape of NPs affect not only their optical properties, but also the ability of these particles to be absorbed by living cells and affect their viability. This feature should also be taken into account when developing plasmonic markers based on NPs of various morphologies [14–16]. Regarding GNSs, there are literature data that they are able to penetrate cells with high efficiency [17,18]. Thus, GNSs are suitable objects for bioimaging using red lasers and, for these reasons, were chosen as the basis for the optical labels studied in this work.

There are two types of GNS synthesis: two-stage grain growth methods [19] and one-stage methods without using the nuclei [20]. The length of the GNS beam strongly depends on the ratio of the used reagents [18], in particular, the higher Au^{3+}/ascorbic acid ratio provides a longer nanostar beam length. In addition, it is important to take into account the stability of the particles, which depends on the method of preparation and the type of stabilizing agent [21], since only systems with long-term aggregative stability can be used for bioimaging. The present work is aimed for obtaining, studying and biological testing of stable optical marks of the „core−shell" type based on ZNZ, which have the most efficient GRS response when excited by a laser with a wavelength from 630 to 660 nm.

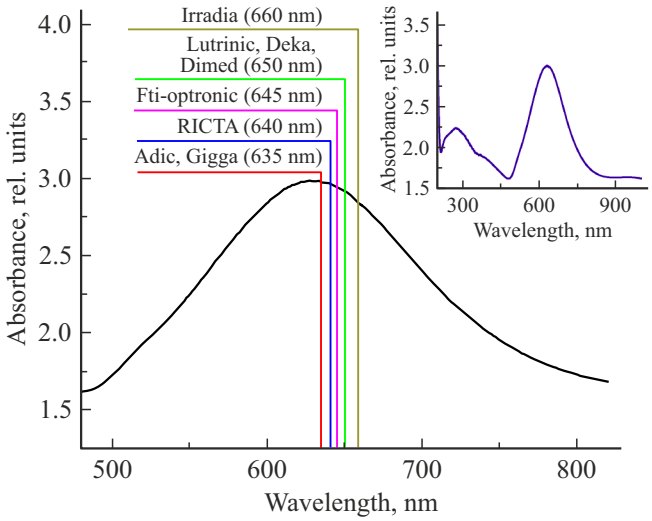

Figure 1. GNS absorption spectrum. The vertical lines indicate the wavelengths of some commonly used medical red lasers.

Experiment procedure

Gold nanostars were obtained by one-stage synthesis by the method of He et al. [22]. Further modification of the GNS included the steps of functionalization with a coloring material, coating with a biocompatible capping, and attachment of the delivery vector to the folic acid receptor. Coating of GNS with a polymer capping was carried out according to the „layer by layer“ method using a polymer in the anionic form of polystyrene sulfonate (PSS) and a polymer in the cationic form of polydiallyldimethylammonium chloride (PDDA). Derivatives of the dye cyanine 5.5 (Cy-5.5) were chosen as Raman markers for the following reasons. The range of their optical absorption corresponds to the absorption region of GNS, which ensures a higher probability of observing resonant Raman scattering. The coloring material was introduced into the polymer capping by adding to the solution before applying the sealing layer of the polymer. To do this, a coloring material solution with a concentration of $1.2 \cdot 10^{-4}$ M was added dropwise to a colloidal solution of GNS with stirring in a ratio of 1 : 20. The immobilization of the coloring material on the NP surface proceeded due to adsorption interactions. The excess of un-adsorbed coloring material was removed by centrifugation. Folic acid was used as a model delivery vector by applying it to the outer polymeric layer of the coated GNSs.

Spectrophotometric analysis of the initial solution of GNS and modified systems based on them was performed on a UV-1800 spectrophotometer (Shimadzu). The spectrum was recorded in the range from 200 to 1100 nm with a step of 1 nm. Quartz cuvettes with an optical path length of 1/cm were used for recording. The baseline was taken from deionized water under the same conditions.

Transmission electron microscopy (TEM) images of GNSs were obtained on Libra 200FE electron microscope (Carl Zeiss) with accelerating voltage of 200 kV. TEM images in scanning mode were recorded from three random areas of the sample. The GNS solution was applied dropwise (10 mkl) onto the surface of carbon films, after which the samples were placed in a dark place to evaporate the solvent in air.

GRS spectra were recorded on a LabRam-HR 800 spectrometer (Horiba Jobin-Yvon). The spectra were excited using a line with a wavelength of 632.8 nm from a He−Ne laser. The laser radiation power was 20 mW when measuring in solution and 2 mW when taking cell samples.

The cytotoxicity test was performed using the tetrazolium coloring material 3-(4,5-dimethylthiazole-2-yl)-2,5-diphenyl-tetrazolium bromide. The PANC-1 cell line was seeded in a 96-well plate with a population of 10,000 cells per well and incubated for 24 h. Solutions of modified GNS prepared in DMEM nutritional medium with atomic gold concentration from 0.05 to 1 mg/l, were added to cells and incubated for 24 h. After that, tetrazolium coloring material was added at a concentration of 0.15 mg/ml and incubated for 1 h. Then, 100 μm of dimethyl sulfoxide was added to each well, and the absorbance was measured at a wavelength of 570 nm.

Results and discussion

Absorption spectra of the GNS under study are presented in Fig. 1. As can be seen, the absorption band covers the range practically from 500 to 800 nm, while the maximum falls at a wavelength of 620 nm. For clarity, in Fig. 1, vertical lines are also drawn, indicating the wavelengths of some used practically red medical lasers. As can be seen, their wavelengths fall on the right shoulder of the GNS absorption band, but are not far from the maximum. This mutual arrangement of the absorption maximum of the metal substrate and the wavelength of the excitation source is considered optimal in SERS spectroscopy and makes it possible to expect the appearance of an intense signal. The use of lasers for observing GRS, with a wavelength slightly longer than the absorption maximum of a metal substrate, is considered more advantageous in comparison with the situation of their absolute coincidence, since it provides the conditions for the most efficient amplification of both exciting and scattered radiation participating in the Raman scattering process [23].

The TEM images of the obtained GNSs are shown in Fig. 2. Each particle consists of a nucleus about 60 nm in diameter and 7−10 short and long rays directed in different directions. The observed morphology correlates well with the recorded absorption spectra. The absence of a pronounced separation into transverse and longitudinal modes of localized plasmon resonance is determined by the relatively symmetric longitudinal dimensions in relation to the width and length of the particles. The presence of rays with a length of 20 to 70 nm leads to a significant shift of absorption to the long-wavelength region in comparison with spherical gold nanoparticles.

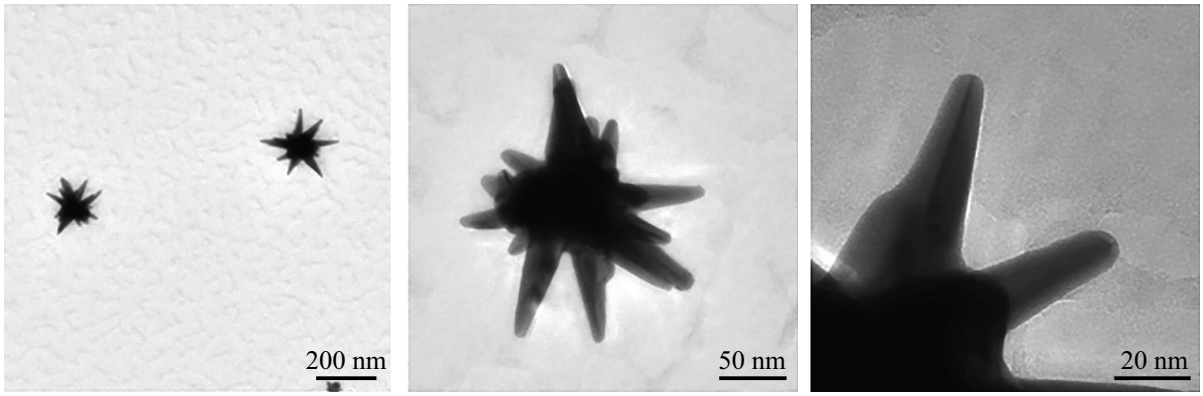

Figure 2. TEM images of the investigated GNSs.

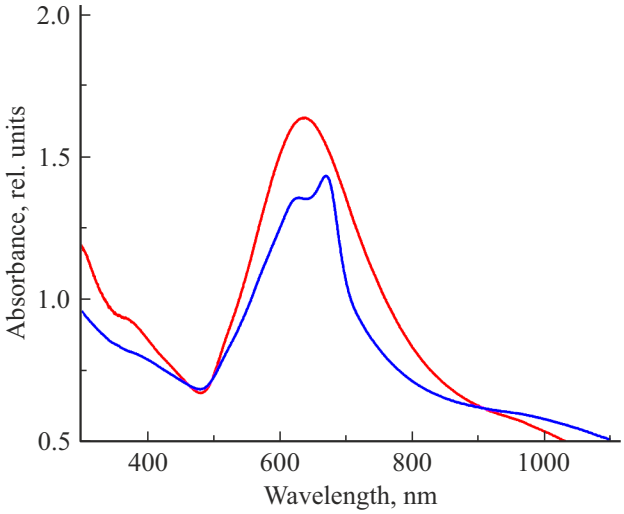

Figure 3. Absorption spectra of GNS after the addition of the coloring material (blue curve) and after the final addition of folic acid (red curve). The spectra are normalized in terms of intensity at a wavelength of 485 nm.

The coating of a metal core with a is often used to functionalize nanoparticles and ensure their aggregative stability in media of complex composition, including those with a high salt background. A similar technique was also applied in the present work with respect to the GNS. To control the functionalization with the dye and monitor the aggregative stability, the absorption spectra were recorded after individual stages of the GNS modifications. The spectra obtained after the addition of the coloring material and after the final stage of addition of folic acid are shown in Fig. 3. A pronounced peak at 671 nm in the spectrum after the addition of the coloring material indicates its successful entry into the particle capping. However, it should be noted that the dye was partially washed out after the subsequent stage of addition of folic acid; the residual content of the dye after all stages of coating was about 40–60% of the initial concentration in the GNS solution. On the whole, the absorption spectra demonstrate a high aggregative stability of the obtained systems, since the maximum of the absorption band of the modified GNS exactly corresponds to the maximum of the absorption band of the initial colloidal solution, which indicates the absence of agglomerates.

The correct choice of molecules that will act as the source of the optical marker signal is an important stage in their development. In the case of using dyes as Raman markers, there is often a problem of a high background fluorescence signal, which can overlap the target Raman signal. Performing of preliminary spectral measurements in the solution phase often helps to predict the optical response. It is for this purpose that the GRS spectra of two Cyanine5.5 derivatives were recorded in the initial GNS solution, which are shown in Fig. 4.

As can be seen, the fluorescent background is present both for the amine derivative Cy-5.5 (black curve) and for the sulfo-activated ester (red curve). However, in the spectrum of the derivative with an amino group, significant characteristic Raman bands from the coloring material appear in the low-frequency region. The observed difference between the two Cyanine5.5 derivatives can be associated with different positions of the emission bands of these compounds and a higher affinity for the surface of the amine derivative. The emission range of the sulfo-activated ester Cyanine-5.5 is in the region of 650–800 nm with a maximum at 700 nm, while the emission range of the amino derivative Cyanine5.5 is in the region of 660–850 nm with a maximum at 710 nm. It would seem that an insignificant difference in the position of the emission bands is decisive for obtaining the GRS signal upon excitation by a helium-neon laser with a wavelength of 632.8 nm. This is especially clearly seen in the GRS spectra correlated with the absolute wavelength scale expressed in nanometers (the upper scale in Fig. 4). A shift of 10 nm to the long wavelength region of the emission band of the amine derivative Cyanine5.5 provides a „window“ in the wavenumber range 0-800 cm-1, in which the fluorescent background is quite low. Thus, any of the components in the region 100–800 cm^{-1} in the GRS spectrum of the amino derivative Cyanine-5.5

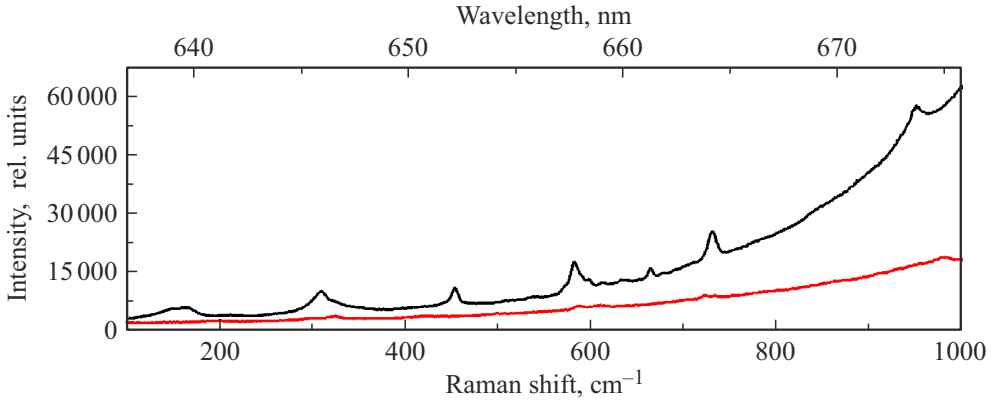

Figure 4. GRS spectra of Cyanine5.5 amine (black curve) and sulfo-Cyanine5.5 activated ester (red curve) adsorbed on GNZ.

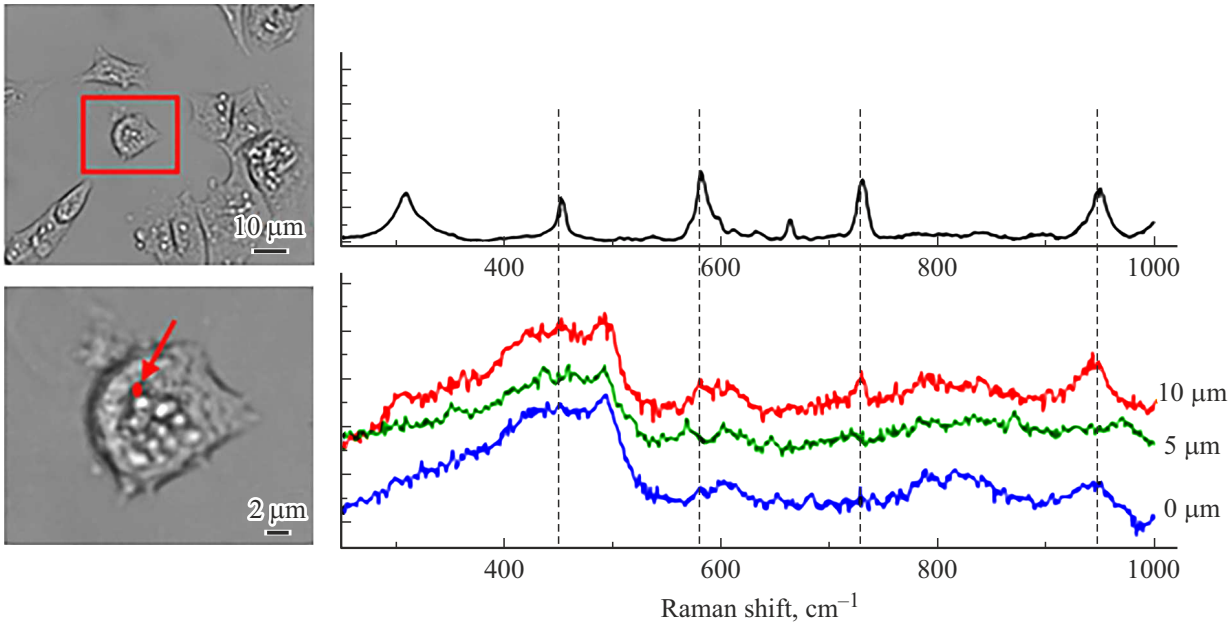

Figure 5. Optical images of a cell sample for which SERS spectra were taken (left); SERS spectra of the amino derivative Cyanine5.5 in GNS solution after baseline subtraction (upper right); GRS spectra of modified GNSs recorded in PANC-1 cells at different depths relative to their surface (bottom right). The red dot on the optical image indicates the area of registration of the GRS spectra inside the cell.

can be used for mapping with GNS-based markers. These bands were used to track modified GNSs in subsequent cell experiments.

The GRS spectra obtained from cell samples after incubation with modified GNSs are shown in Fig. 5. A weak but characteristic signal in the region of 100–1000 cm^{-1} was found for all cells (Fig. 5). The GRS spectra recorded with height scanning were measured to verify the intracellular location of GNSs. The observed increase in the intensity of the signal of the amino derivative Cyanine-5.5 as the focus shifts from the surface to the bulk of the cell indicates that the particles are inside it, and not on the surface. The observed weaker signal in comparison with the GNS spectra in solution is associated with both the lower power of the laser radiation used and the lower content of particles in the cell.

The cytotoxicity of any optical markers used for bioimaging should be tested prior to animal testing and subsequent use. Therefore, an MTT test for the folate receptor of the positive PANC-1 cell line (Fig. 6). was performed with systems based on GNS. As can be seen from the figure, cell viability in the presence of GNS corresponds within the error of viability of control samples. Based on this, it can be said that the studied GNS with folic acid as a delivery vector do not exhibit toxic properties in the concentration range of atomic gold from 0.05 to 1 mg/l. The result obtained opens the prospect of further testing of systems based on GNS in animals and a possible transition to preclinical trials.

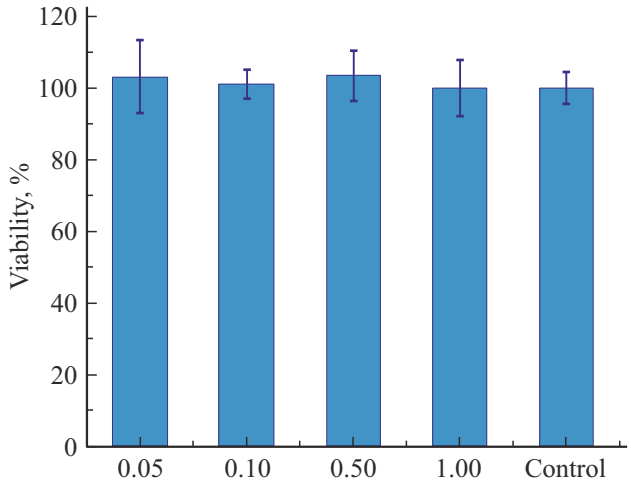

Figure 6. Viability of the PANC-1 cell line after incubation with modified GNSs for 24 h. On the abscissa axis, the concentrations of atomic gold are indicated.

Conclusions

In this work, optical markers for bioimaging by the GRS method based on GNS and cyanine dyes, excited in the red range of the electromagnetic spectrum, were obtained. The plasmonic core of the marker provides a pronounced GRS signal from the dye located in the polymer shell. When excited by a helium-neon laser, the working spectral range of the marker, not overlapped by fluorescence, is $100-1000\,cm^{-1}$, in which five Cyanine-5.5 vibrational bands can be used as a characteristic signal for mapping cells. The GRS spectra recorded after particle incubation with the PANC-1 cell line confirm the intracellular localization of the labels. The test for cytotoxicity showed that GNS optical markers s do not have a toxic effect in the concentration range from 0.05 to 1 mg/l in terms of atomic gold. On the whole, the results of this work demonstrate the high potential of using optical labels based on GNS for diagnostic purposes using red medical lasers.

Acknowledgments

The authors are grateful to the Resource Centers of St. Petersburg State University: „Optical and laser methods for studying matter“, „Methods for analyzing the composition of matter“, „Interdisciplinary Center for Nanotechnology“ and „Center for Molecular and Cellular Technologies“.

Funding

The study was supported in part by St. Petersburg State University, project № 92350587 (synthesis and modification of gold nanoparticles, TEM and GRS measurements) and with partial financial support from the Russian Science Foundation, grant № 22-73-10052, https ://rscf.ru/project/22-73-10052/ (MTT testing with cell lines).

Conflict of interest

The authors declare that they have no conflict of interest.

References

[1] R. Steiner. Laser-Tissue Interactions, Laser and IPL Technology in Dermatology and Aesthetic Medicine, 23–36 (2011). DOI: 10.1007/978-3-642-03438-1_2
[2] Q. Peng, A. Juzeniene, J. Chen, L.O. Svaasand, T. Warloe, K.E. Giercksky, J. Moan. Rep. Progr. Phys., **71**(5), 056701 (2008). DOI: 10.1088/0034-4885/71/5/056701
[3] M.K. Yeh, C.C. Chen, D.S. Hsieh, K.J. Huang, Y.L. Chan, P.D. Hong, C.J. Wu. Development and Therapy, 459 (2014). DOI: 10.2147/DDDT.S58414
[4] Y. Wu, Y. Feng, X. Li. J. Colloid and Interface Sci., **611**, 287–293 (2022). DOI: 10.1016/j.jcis.2021.12.039
[5] W. Zhang, L. Jiang, J. A. Piper, Y. Wang. J.Analysis and Testing, **2**(1), 26–44 (2018). DOI: 10.1039/c4sc02600d
[6] A.N. Spitsyn, D.V. Utkin, O.S. Kuznetsov, P.S. Erokhin, N.A. Osina, V.I. Kochubei Opt. i spektr., **129** (1), 100 (2021) (in Russian). DOI:10.21883/OS.2021.01.50446.200-20
[7] S. Wagner, T. Dieing, A. Centeno, A. Zurutuza, A.D. Smith, M. Östling, S. Kataria, M.C. Lemme. Nano Lett., **17**(3), 1504–1511 (2017). DOI: 10.1021/acs.nanolett.6b04546
[8] T. Böhm, R. Moroni, S. Thiele. J. Raman Spectr., **51**(7), 1160–1171 (2020). DOI: 10.1002/jrs.5878
[9] X. Luo, D. Chen, Y. Zhan, J. Liang, X. Chen. Proc. SPIE108 **90**, 1089009 (2019). DOI: 10.1117/12.2508455
[10] A.B. Bucharskaya, G.N. Maslyakova, M.L. Chekhonatskaya, N.B. Zakharova, G.S. Terentyuk, N.A. Navolokin, B.N. Khlebtsov, N.G. Khlebtsov, V.D. Genin, A.N. Bashkatov, E.A. Genina, V.V. Tuchin. Opt. i spektr., **128** (6), 846 (2020) (in Russian). DOI:10.21883/OS.2020.06.49419.34-20
[11] M. Chirumamilla, A. Gopalakrishnan, A. Toma, R. Proietti Zaccaria, R. Krahne. Nanotechnology, **25**(23), 235303 (2014). DOI: 10.1088/0957-4484/25/23/235303
[12] A. Yoshida, N. Uchida, N. Kometani. Langmuir, **25**(19), 11802–11807 (2009). DOI: 10.1021/la901431r
[13] J.A. Jenkins, T.J. Wax, J.Zhao. J. Chem. Education, **94**(8), 1090–1093 (2017). DOI: 10.1021/acs.jchemed.6b00941
[14] B.D. Chithrani, A.A. Ghazani, W.C. Chan. Nano Lett., **6**(4), 662–668 (2006). DOI: 10.1021/nl052396o
[15] I. Canton, G. Battaglia. Chem. Soc. Rev., **41**(7), 2718 (2012). DOI: 10.1039/c2cs15309b
[16] N.M. Schaeublin, L.K. Braydich-Stolle, E.I. Maurer, K. Park, R.I. McCuspie, A.R. Afrooz, R.A. Vaia, N.B. Saleh, S.M. Hussain. Langmuir, **28**(6), 3248–3258 (2012). DOI: 10.1021/la204081m
[17] Q. Wei, H.M. Song, A.P. Leonov, J. A. Hale, D. Oh, Q.K. Ong, K. Ritchie, A. Wei. J. Am. Chem. Soc., **131**(28), 9728–9734 (2009). DOI: 10.1021/ja901562j
[18] A. Guerrero-Martínez, S. Barbosa, I. Pastoriza-Santos, L.M. Liz-Marzán. Current Opinion in Colloid & Interface Science, **16**(2), 118–127 (2011). DOI: 10.1016/j.cocis.2010.12.007

[19] S. He, M.W. Kang, F.J. Khan, E.K. Tan, M.A. Reyes, J.C. Kah. J. Optics, **17**(11), 114013 (2015). DOI: 10.1088/2040-8978/17/11/114013
[20] M.S. Verma, P.Z. Chen, L. Jones, F.X. Gu. RSC Adv., **4**(21), 10660–10668 (2014). DOI: 10.1039/C3RA46194G
[21] Y. Xia, X. Xia, H.C. Peng. J. Am. Chem. Soc., **137**(25), 7947–7966 (2015). DOI: 10.1021/jacs.5b04641
[22] S. He, M.W. Kang, F.J. Khan, E.K. Tan, M.A. Reyes, J.C. Kah. J. Optics, **17**(11), 114013 (2015). DOI: 10.1088/2040-8978/17/11/114013
[23] B. Sharma, R.R. Frontiera, A.I. Henry, E. Ringe, R.P. Van Duyne. Mater. Today, **15**(1–2), 16–25 (2012).